A comparative study of the magnetic properties of the 1/1 approximant $Ag_{50}In_{36}Gd_{14}$ and the icosahedral quasicrystal $Ag_{50}In_{36}Gd_{14}$

2009 J. Phys.: Condens. Matter 21 436007

(http://iopscience.iop.org/0953-8984/21/43/436007)

J. Phys.: Condens. Matter **21** (2009) 436007 (10pp) doi:10.1088/0953-8984/21/43/436007

A comparative study of the magnetic properties of the 1/1 approximant $Ag_{50}In_{36}Gd_{14}$ and the icosahedral quasicrystal $Ag_{50}In_{36}Gd_{14}$

P Wang[1], Z M Stadnik[1], K Al-Qadi[1] and J Przewoźnik[2]

[1] Department of Physics, University of Ottawa, Ottawa, ON, K1N 6N5, Canada
[2] Solid State Physics Department, Faculty of Physics and Applied Computer Science, AGH University of Science and Technology, 30-059 Kraków, Poland

E-mail: stadnik@uottawa.ca

Received 9 August 2009, in final form 24 September 2009
Published 8 October 2009
Online at stacks.iop.org/JPhysCM/21/436007

Abstract

We report on measurements of the dc and ac magnetic susceptibility, ^{155}Gd Mössbauer spectra, and specific heat of the 1/1 approximant $Ag_{50}In_{36}Gd_{14}$, and of the ac magnetic susceptibility of the icosahedral quasicrystal $Ag_{50}In_{36}Gd_{14}$. These alloys are shown to be spin glasses. For the icosahedral quasicrystal $Ag_{50}In_{36}Gd_{14}$, spin freezing occurs at $T_f = 4.3$ K, and the frequency dependence of T_f is well accounted for by the Vogel–Fulcher and power laws. Spin freezing in the 1/1 approximant $Ag_{50}In_{36}Gd_{14}$ occurs in two stages: at $T_{f_1} = 3.7$ K, Gd spins develop short-range correlations but continue to fluctuate, and then long-range freezing is achieved at $T_{f_2} = 2.4$ K. The frequency dependences of T_{f_1} and T_{f_2} can be accounted for by means of the Vogel–Fulcher law and the critical slowing down dynamics. It is shown that the spin freezing in both alloys is a nonequilibrium phenomenon rather than a true equilibrium phase transition. The ^{155}Gd Mössbauer spectra of the 1/1 approximant $Ag_{50}In_{36}Gd_{14}$ confirm that the Gd spins are frozen at 1.5 K and are fluctuating at 4.6 K. The magnetic specific heat exhibits a maximum at a temperature that is 30% larger than T_{f_1}, but the temperature derivative of the magnetic entropy peaks at T_{f_1}. The Debye temperature of the 1/1 approximant $Ag_{50}In_{36}Gd_{14}$ is 199(1) K as determined from the Mössbauer data, and 205(2) K as determined from the specific heat data.

(Some figures in this article are in colour only in the electronic version)

1. Introduction

Quasicrystals (QCs) are a new form of solid which differs from the other two known forms, crystalline and amorphous, by possessing a new type of long-range translational order, quasiperiodicity, and a noncrystallographic orientational order associated with classically forbidden symmetry axes [1]. A central problem in condensed-matter physics is determining whether quasiperiodicity leads to physical properties which are significantly different from those of crystalline and amorphous materials of the same/similar compositions.

The discovery of the first binary icosahedral (i-)QCs $YbCd_{5.7}$ and $CaCd_{5.7}$ by Tsai *et al* [2] has led to the finding of many ternary i-QCs by total or partial replacement of Yb or Ca and Cd with other metallic elements. In particular, by replacing Yb with rare-earth (RE) elements and Cd with Ag and In, a series of new Ag–In–RE i-QCs was synthesized [3, 4]. Cubic crystalline alloys $YbCd_6$ and $CaCd_6$ are 1/1 approximants [5] to the i-QCs $YbCd_{5.7}$ and $CaCd_{5.7}$, respectively [6, 7]. A similar replacement in $YbCd_6$ of Yb with RE elements and Cd with Ag and In has led to the discovery of ternary Ag–In–RE 1/1 approximants to the Ag–In–RE i-QCs [4, 8]. The availability of icosahedral and 1/1 approximant Ag–In–RE alloys of the same composition allows for a study of the influence of quasiperiodicity on the physical properties of these alloys. In this paper, we report on structural, magnetic, ^{155}Gd Mössbauer spectroscopy (MS), and specific heat studies of the two alloys of the same composition:

the i-QC $Ag_{50}In_{36}Gd_{14}$ and its 1/1 crystalline approximant $Ag_{50}In_{36}Gd_{14}$.

2. Experimental methods

The i-QC $Ag_{50}In_{36}Gd_{14}$ was synthesized as described earlier [9]. To synthesize the 1/1 approximant $Ag_{50}In_{36}Gd_{14}$, starting elements in the form of Ag shots (purity, 99.99%), In shots (purity, 99.999%), and Gd chunks (purity, 99.9%) were used as received. Appropriate amounts of these elements corresponding to the composition $Ag_{50}In_{36}Gd_{14}$ were weighed (±0.1 mg) and weld-sealed under an argon atmosphere into a tantalum container. The container was in turn held within an evacuated SiO_2 jacket to avoid oxidation in air. The mixture was melted using an induction furnace.

X-ray diffraction measurements were performed at 298 K in Bragg–Brentano geometry using a PANanalytical X'Pert scanning diffractometer, using Cu Kα radiation. The Kβ line was eliminated by using a Kevex PSi2 Peltier-cooled solid-state Si detector. In order to avoid deviation from intensity linearity of the solid-state Si detector, its parameters and the parameters of the diffractometer were chosen in such a way as to limit the count rate from the most intense Bragg peaks to less than 9000 counts s^{-1} [10].

The dc magnetic susceptibility was measured with a Quantum Design (QD) Magnetic Property Measurement System at various magnetic fields in the temperature range 2.0–300 K. The ac magnetic susceptibility data were collected using a QD Physical Property Measurement System (PPMS) between 2.0 and 30 K in a 1 Oe ac magnetic field and zero external magnetic field for frequencies varying from 20 Hz to 10 kHz. The specific heat data in the temperature range 2.0–300 K were collected using the same QD PPMS via the relaxation method.

The ^{155}Gd Mössbauer measurements were conducted using a standard Mössbauer spectrometer operating in a sine mode and a source of ^{155}Eu(SmPd$_3$). The source was kept at the same temperature as the absorber. The spectrometer was calibrated with a Michelson interferometer [11], and the spectra were folded. The Mössbauer absorber was made of pulverized material pressed into a pellet which was then put into an Al disk container of thickness of 0.008 mm to ensure a uniform temperature over the whole sample. The surface density of the Mössbauer absorber of the 1/1 approximant $Ag_{50}In_{36}Gd_{14}$ was 356 mg cm^{-2}. The 86.5 keV γ-rays were detected with a 2.5 cm NaI(Tl) scintillation detector covered with a 0.6 mm Pb plate to cut off the 105.3 keV γ-rays emitted from the source.

The Mössbauer spectra were analyzed by means of a least-squares fitting procedure which entailed calculations of the positions and relative intensities of the absorption lines by numerical diagonalization of the full hyperfine interaction Hamiltonian. In the principal axis coordinate system of the electric field gradient (EFG) tensor, the Hamiltonian can be written as [12]

$$\hat{H} = g\mu_B H_{hf}\left[\hat{I}_z\cos\theta + \tfrac{1}{2}(\hat{I}_+ e^{-i\phi} + \hat{I}_- e^{i\phi})\sin\theta\right] + \frac{eQV_{zz}}{4I(2I-1)}\left[3\hat{I}_z^2 - I(I+1) + \frac{\eta}{2}(\hat{I}_+^2 + \hat{I}_-^2)\right], \quad (1)$$

where g is a nuclear g-factor of a nuclear state, μ_B is the nuclear Bohr magneton, H_{hf} is the hyperfine magnetic field at a nuclear site, Q is the quadrupole moment of a nuclear state, I is the nuclear spin, V_{zz} is the z component of the EFG tensor, η is the asymmetry parameter defined as $\eta = |(V_{xx} - V_{yy})/V_{zz}|$ (if the principal axes are chosen such that $|V_{xx}| < |V_{yy}| < |V_{zz}|$, then $0 \leqslant \eta \leqslant 1$), θ is the angle between the direction of H_{hf} and the V_{zz}-axis, ϕ is the angle between the V_{xx}-axis and the projection of H_{hf} onto the xy plane, and the $\hat{I}_z$, $\hat{I}_+$, and $\hat{I}_-$ operators have their usual meaning. During the fitting procedure, the g-factor and the quadrupole moment ratios for ^{155}Gd ($I_g = 3/2$, $I_{ex} = 5/2$) were constrained to $g_{ex}/g_g = 1.235$ and $Q_{ex}/Q_g = 0.087$, respectively [13]. The interference factor ξ for the E1 transition of 86.5 keV in ^{155}Gd was fixed to the value of 0.0520 which was derived from the fit of the ^{155}Gd Mössbauer spectrum of $GdFe_2$ at 4.2 K [14].

The resonance line shape of the Mössbauer spectra was described using a transmission integral formula [15]. In addition to the hyperfine parameters, only the absorber Debye–Waller factor f_a and the absorber linewidth Γ_a were fitted as independent parameters. The source linewidth $\Gamma_s = 0.334$ mm s^{-1} and the background-corrected Debye–Waller factor of the source f_s^* [15], which were derived from the fit of the ^{155}Gd Mössbauer spectrum of $GdFe_2$ at 4.2 K [14], were used. The ^{155}Eu(SmPd$_3$) source at 1.5 K emits a broadened emission line; from the fit of the ^{155}Gd Mössbauer spectrum of $GdFe_2$ at 1.5 K we found that $\Gamma_s = 0.708$ mm s^{-1} [14].

3. Results and discussion

3.1. Structural characterization

All major Bragg peaks of the XRD spectrum of the i-QC $Ag_{50}In_{36}Gd_{14}$ could be indexed to a simple icosahedral (SI) six-dimensional Bravais lattice [9]. The value of the six-dimensional hypercubic lattice constant a_{6D} for this i-QC is 7.805 Å [9].

The 1/1 approximant $Ag_{50}In_{36}Gd_{14}$ crystallizes in the $YbCd_6$-type crystal structure [7] with the space group $Im\bar{3}$ (No. 204). There are 24 formula units of $(Ag, In)_6Gd$ per unit cell. The x-ray powder diffraction pattern of the 1/1 approximant $Ag_{50}In_{36}Gd_{14}$ is shown in figure 1. In the Rietveld refinement, the atomic positions for the Ag, In, and Gd sites and their occupancies were fixed to the positions and occupancies, respectively, for the Cd and Gd sites in the $GdCd_6$ approximant [7]. The Rietveld refinement of the x-ray powder diffraction data was performed (figure 1), yielding the lattice parameter $a = 15.202(1)$ Å. The reliability factors [16] achieved are $R_{exp} = 6.2\%$, $R_p = 17.2\%$, and $\chi^2 = 9.4$. The sample studied contains traces of second phases of Ag_3In (space group $P6_3/mmc$) in the amount of 5.2(6) wt% and of Gd (space group $Fm\bar{3}m$) in the amount of 0.6(2) wt%, as determined from the Rietveld refinement of the XRD pattern (figure 1).

The lattice constant a of a 1/1 approximant to an i-QC is related to the six-dimensional hypercubic lattice constant a_{6D} of the i-QC via the relation $a = \sqrt{\frac{2}{2+\tau}}(1+\tau)a_{6D}$, where τ is the golden mean ($\tau = (1+\sqrt{5})/2$) [17]. From the value

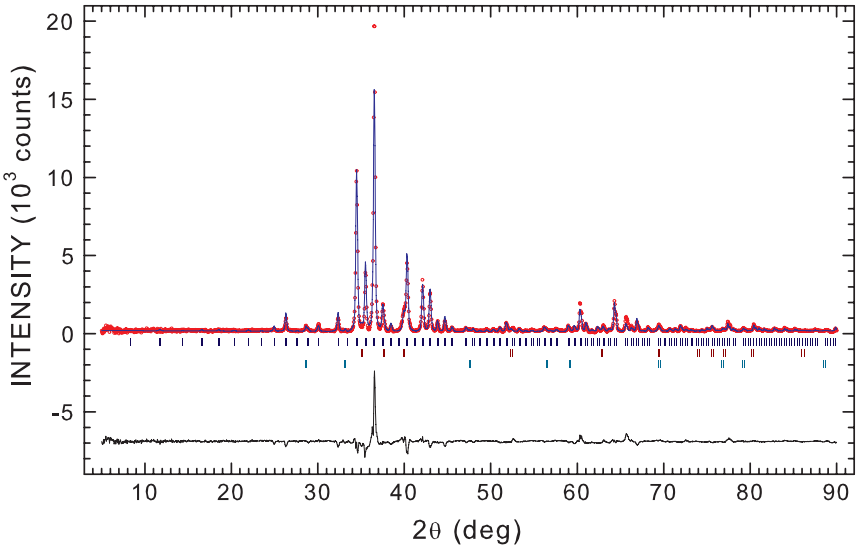

Figure 1. The x-ray diffraction spectrum of the 1/1 approximant $Ag_{50}In_{36}Gd_{14}$ at 298 K. The experimental data are denoted by open circles, while the line through the circles represents the results of the Rietveld refinement. The upper set of vertical bars represents the Bragg peak positions corresponding to the principal $Ag_{50}In_{36}Gd_{14}$ phase, while the lower two sets refer to the positions of the minor impurity phases of Ag_3In (space group $P6_3/mmc$) and Gd (space group $Fm\bar{3}m$). The lower solid line represents the difference curve, between experimental and calculated spectra.

$a_{6D} = 7.805$ Å for the i-QC $Ag_{50}In_{36}Gd_{14}$, one would expect $a = 15.192$ Å, which is in good agreement with the value of 15.202 Å obtained from the Rietveld refinement.

3.2. Magnetic measurements

3.2.1. The dc magnetic susceptibility. The magnetic susceptibility χ of the i-QC $Ag_{50}In_{36}Gd_{14}$ showed irreversibility between field-cooled (FC) and zero-field-cooled (ZFC) conditions, thus demonstrating that this QC is a spin glass, with the spin freezing temperature $T_f = 4.25(5)$ K [9].

The temperature dependence of χ for the 1/1 approximant $Ag_{50}In_{36}Gd_{14}$ measured in an applied magnetic field of 50 Oe is shown in figure 2(a). The sample was field cooled to 2.0 K and the measurement was performed while warming the sample up to 300 K. The $\chi(T)$ curve exhibits a definite peak at 3.6(1) K indicating magnetic ordering. The $\chi(T)$ data above 70 K could be fitted to a modified Curie–Weiss law

$$\chi = \chi_0 + \frac{C}{T - \Theta_p}, \tag{2}$$

where χ_0 is the temperature-independent magnetic susceptibility, C is the Curie constant, and Θ_p is the paramagnetic Curie temperature. The Curie constant can be expressed as $C = \frac{N\mu_{eff}^2}{3k_B}$, where N is the concentration of magnetic atoms per unit mass, μ_{eff} is the effective magnetic moment, and k_B is the Boltzmann constant. Figure 2(b) shows the inverse magnetic susceptibility corrected for the contribution χ_0 as $(\chi - \chi_0)^{-1}$ versus temperature; the validity of the modified Curie–Weiss law is evident. The values of χ_0, C, and Θ_p obtained from the fit are, respectively, $8.94(48) \times 10^{-6}$ emu g^{-1} ($7.49(40) \times 10^{-3}$ emu/(mol Gd)), $8.71(20) \times 10^{-3}$ emu K g^{-1}, and $-55.9(2)$ K. This value of C corresponds to $\mu_{eff} = 7.64(9)\ \mu_B$ per Gd atom.

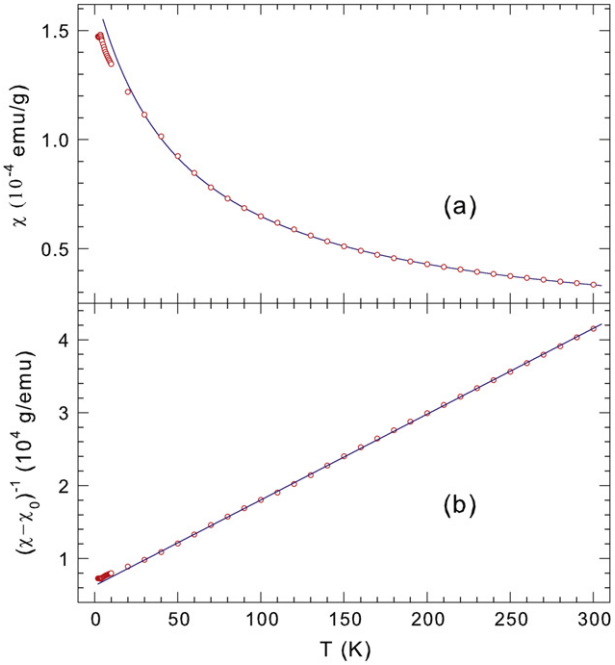

Figure 2. (a) The temperature dependence of the magnetic susceptibility of the 1/1 approximant $Ag_{50}In_{36}Gd_{14}$, measured in an external magnetic field of 50 Oe. The solid line is the fit to equation (2) in the temperature range 70–300 K, as explained in the text. (b) The inverse magnetic susceptibility corrected for the contribution χ_0, $(\chi - \chi_0)^{-1}$, versus temperature T for the 1/1 approximant $Ag_{50}In_{36}Gd_{14}$. The solid line is the fit to equation (2).

The temperature-independent magnetic susceptibility χ_0 includes contributions from the Pauli susceptibility of conduction electrons and the diamagnetic susceptibility of core electrons, $\chi_0 = \chi_P + \chi_d$. The latter can be estimated as a

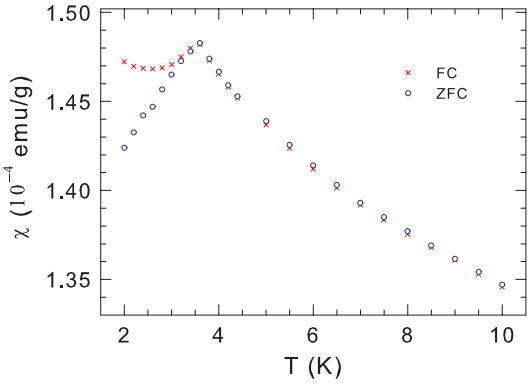

Figure 3. The temperature dependence of the ZFC and FC magnetic susceptibility of the 1/1 approximant $Ag_{50}In_{36}Gd_{14}$, measured in an external magnetic field of 50 Oe.

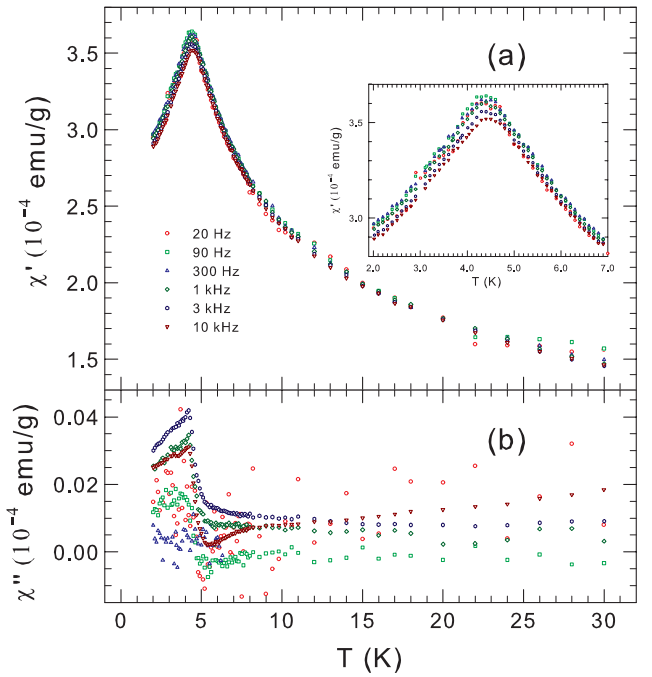

Figure 4. The temperature dependence of the in-phase magnetic susceptibility χ' (a) and out-of-phase magnetic susceptibility χ'' (b) measured for different applied frequencies from 20 Hz to 10 kHz for the i-QC $Ag_{50}In_{36}Gd_{14}$. The inset in (a) is a magnification around the maximum in χ'.

weighted mean of the susceptibilities of the constituents of the alloy [18], and is thus $\chi_d = -1.55 \times 10^{-4}$ emu/(mol Gd). The value of χ_P is therefore $7.65(40) \times 10^{-3}$ emu/(mol Gd). The derived value of χ_P is about two times larger than that found for other single-crystalline Gd-containing alloys [19]. The large value of χ_P found here results most probably from the contribution to χ_0 from the small amount of ferromagnetic Gd impurity present in the studied sample.

For a free Gd^{3+} ion (electronic configuration $^8S_{7/2}$), the theoretical value of $\mu_{\rm eff}^{\rm th} = g\mu_B\sqrt{J(J+1)}$ is 7.94 μ_B [20]. The fact that the experimental value $\mu_{\rm eff} = 7.64(9)$ μ_B is close to the theoretical value of 7.94 μ_B confirms that the magnetic moment is localized on the Gd^{3+} ions and that, as expected, Ag and In atoms carry no magnetic moment. The negative value of Θ_p indicates the predominantly antiferromagnetic interaction between the Gd^{3+} spins.

To determine the nature of the magnetic transition at 3.6 K, we measured the temperature dependence of the ZFC and FC magnetic susceptibility between 2 and 10 K in an applied magnetic field of 50 Oe (figure 3). The occurrence of a bifurcation between the ZFC and FC data at the freezing temperature $T_f = 3.6(1)$ K is evident. Above T_f the ZFC and FC data are essentially identical. Such a behavior of the ZFC and FC susceptibility data is characteristic of a spin glass [21].

The occurrence of spin-glass behavior requires both randomness and frustration [21, 22]. The frustration parameter f, defined as $f = -\Theta_p/T_f$ [23], is an empirical measure of frustration. Compounds with $f > 10$ are categorized as strongly geometrically frustrated compounds [23]. The value of f for the 1/1 approximant $Ag_{50}In_{36}Gd_{14}$ is 15.5(1.1). The value of f for the i-QC $Ag_{50}In_{36}Gd_{14}$ is 8.7 [9]. Thus the 1/1 approximant $Ag_{50}In_{36}Gd_{14}$ belongs to a category of strongly geometrically frustrated magnets.

3.2.2. The ac magnetic susceptibility. Figure 4 shows the temperature dependence of the in-phase component χ' and the out-of-phase component χ'' of the ac magnetic susceptibility of the i-QC $Ag_{50}In_{36}Gd_{14}$ for different frequencies between 20 Hz and 10 kHz. As the magnitude of χ'' is typically a few per cent of the value of χ' for spin glasses [21], this leads to a reduced signal-to-noise ratio in the χ'' data. Both χ' and χ'' curves show maxima whose amplitudes and positions depend on the frequency f of the applied ac magnetic field. With increasing frequency, the peak positions are shifted to higher temperatures, the peak intensity of $\chi'(T)$ decreases, and the peak intensity of $\chi''(T)$ increases. These features are typical for canonical spin glasses [21]. The position of the sharp peak in $\chi'(T)$ can be used to define T_f. Below the maximum in $\chi'(T)$, the magnitude of χ' is frequency dependent, but it becomes independent of frequency at temperatures just above T_f. This behavior is qualitatively similar to that of canonical spin glasses [21]. The out-of-phase component χ'' is vanishing above T_f, but is non-zero for temperatures just below T_f, which implies dissipation not only at the freezing transition but also for temperatures below it, a common feature of spin glasses [21].

The temperature (T_f) of the maximum in $\chi'(T)$ (figure 4(a)) was determined from a curve fitting procedure, where the variation $\chi'(T)$ near T_f was assumed to be a Gaussian function. The frequency dependence of T_f is shown in figure 5. A quantitative measure of the change of the freezing temperature with frequency in spin glasses is represented by the relative change in T_f per decade change in f defined as [21]

$$K = \frac{\Delta T_f}{T_f \Delta \log f}. \qquad (3)$$

From a linear fit of the data in figure 5, and using the average value of $T_f = 4.42$ K for the range of frequencies used, one finds that $K = 0.010(2)$. This value is a factor of about 2 greater than that found for such canonical spin glasses as $Cu_{1-x}Mn_x$ ($K = 0.005$), $Au_{1-x}Mn_x$ ($K = 0.0045$), and

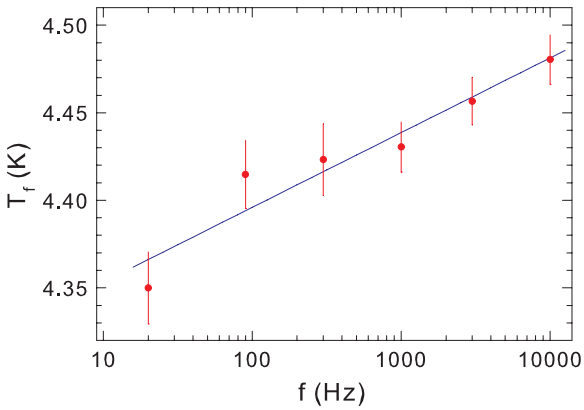

Figure 5. The frequency dependence of the freezing temperature T_f for the i-QC $Ag_{50}In_{36}Gd_{14}$. The solid line is the best linear fit to the T_f data.

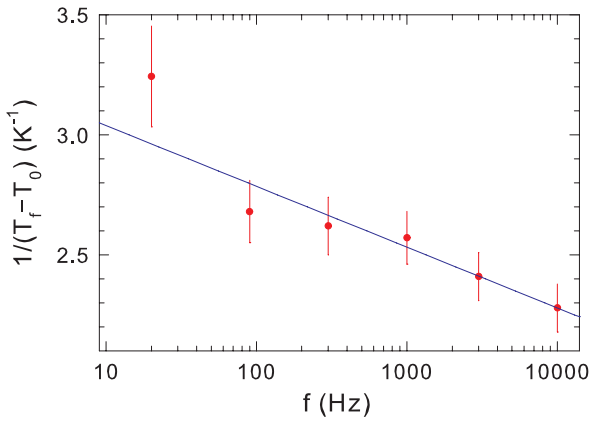

Figure 6. The frequency dependence of the freezing temperature T_f for the i-QC $Ag_{50}In_{36}Gd_{14}$. The solid line is the best fit to equation (4).

$Ag_{1-x}Mn_x$ ($K = 0.006$), but comparable to that of several other canonical spin glasses such as $Au_{1-x}Fe_x$ ($K = 0.010$) and $Pd_{1-x}Mn_x$ ($K = 0.013$) [21]. We note that the value of K reported for another i-QC $Tb_9Mg_{34}Zn_{57}$ is 0.049 [24].

There are essentially two different possible interpretations of the spin-glass freezing process. The first one assumes the existence of spin clusters and, in this case, the freezing is a nonequilibrium phenomenon [25]. The second interpretation assumes the existence of a true equilibrium phase transition at a finite temperature [26]. For magnetically interacting clusters, the frequency dependence of T_f is described by the phenomenological Vogel–Fulcher law [21, 25]

$$f = f_0 \exp[-E_a/k_B(T_f - T_0)], \tag{4}$$

where f_0 is a characteristic frequency, E_a is the activation energy, and T_0 is the Vogel–Fulcher temperature which is a measure of the strength of interaction between clusters in the spin glass [27]. Equation (4) implies a linear dependence of $1/(T_f - T_0)$ with $\log(f)$. The best fit of the $T_f(f)$ data to equation (4) (figure 6), assuming $f_0 = 1 \times 10^{13}$ Hz as typically observed for other spin glasses [25], yields $E_a/k_B = 9.09(38)$ K and $T_0 = 4.04(2)$ K. For this fit, the coefficient of determination [28] $r^2 = 0.9981$. Similarly to what was observed for other spin glasses [25], we find $T_0 < E_a/k_B$.

In the second interpretation of the spin freezing phenomenon, the characteristic relaxation time $\tau = 1/f$ of magnetic moments will show a critical slowing down when approaching T_f from above, characterized by a power law $\tau \propto \xi^z$, where ξ is the correlation length and z is the dynamic scaling exponent [29]. The correlation length ξ itself is related to the reduced temperature $t = (T_f - T_c)/T_c$ as $\xi \propto t^{-\nu}$, where T_c is the phase transition temperature and ν is the critical correlation length exponent [29]. Therefore, the temperature dependence of f obeys the power-law divergence [21, 29]

$$f = f_0 \left(\frac{T_f - T_c}{T_c}\right)^{z\nu}, \qquad T_f > T_c, \tag{5}$$

where f_0 is the microscopic relaxation time. The best fit of the $T_f(f)$ data in figure 7 to equation (5), assuming $f_0 = 1 \times 10^{13}$ Hz as typically observed for other spin glasses [25], gives $T_c = 4.35(3)$ K and $z\nu = 5.97(10)$. For this fit, $r^2 = 0.9907$. The value of $z\nu$ obtained falls in the range 4–12 of $z\nu$ values found for many different spin glasses [21, 30].

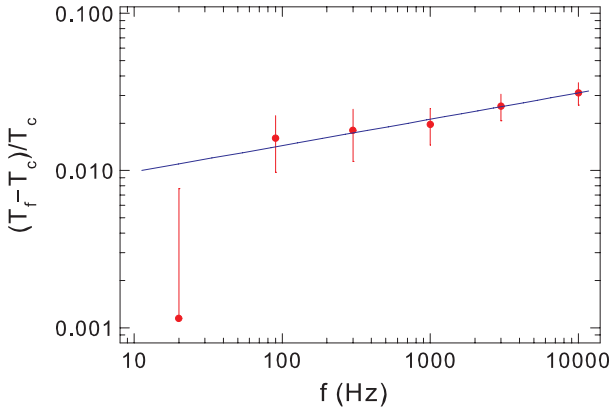

Figure 7. The frequency dependence of the freezing temperature T_f for the i-QC $Ag_{50}In_{36}Gd_{14}$. The solid line is the best fit to equation (5).

The value of r^2 corresponding to the fit of the $T_f(f)$ data to equation (4) is larger than that corresponding to the fit to equation (5), which indicates that the spin freezing in the i-QC $Ag_{50}In_{36}Gd_{14}$ is a nonequilibrium phenomenon rather than a phase transition.

The temperature dependence of χ' for the 1/1 approximant $Ag_{50}In_{36}Gd_{14}$ for selected frequencies between 300 Hz and 10 kHz is shown in figure 8. The $\chi'(T)$ curve shows two maxima: one at ≈3.6 K and the other at ≈2.4 K. The maximum at ≈3.6 K is similar to that observed in the dc $\chi(T)$ data (figure 3). The amplitudes and positions of these two maxima depend on the frequency f of the applied ac magnetic field. The position of the maximum in $\chi'(T)$ is used to define T_f. It thus appears that the spin freezing in the 1/1 approximant $Ag_{50}In_{36}Gd_{14}$ is a two-stage process: it starts at $T_{f_1} \approx 3.6$ K and is completed at $T_{f_2} \approx 2.4$ K.

Figure 9 shows the temperature dependence of χ'' for the 1/1 approximant $Ag_{50}In_{36}Gd_{14}$ for selected frequencies

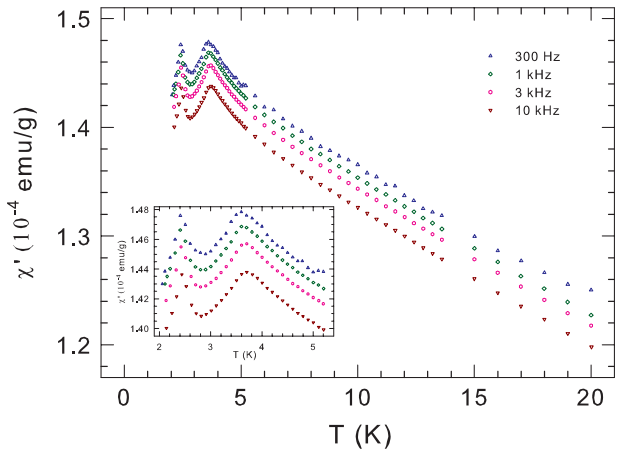

Figure 8. The temperature dependence of the in-phase magnetic susceptibility χ' measured for different applied frequencies from 300 Hz to 10 kHz for the 1/1 approximant $Ag_{50}In_{36}Gd_{14}$. The inset shows a magnification of the low-temperature region.

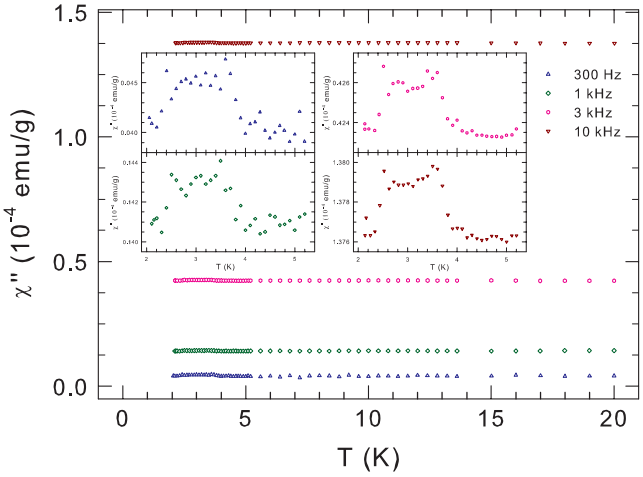

Figure 9. The temperature dependence of the out-of-phase magnetic susceptibility χ'' measured for different applied frequencies from 300 Hz to 10 kHz for the 1/1 approximant $Ag_{50}In_{36}Gd_{14}$. The insets show a magnification of the low-temperature region.

between 300 Hz and 10 kHz. One can clearly observe a sudden increase of χ'' above its background value near T_{f_1} and a sudden decrease of χ'' back to its background value near T_{f_2}.

The temperatures T_{f_1} and T_{f_2} of the maxima in χ' (figure 8) were determined using a curve fitting procedure. The frequency dependence of T_{f_1} and T_{f_2} is shown in figure 10. From a linear fit of the data in figure 10, and using the average values of $T_{f_1} = 3.70$ K and $T_{f_2} = 2.44$ K for the range of frequency used, we find from equation (3) that $K_1 = 9.4(1.5) \times 10^{-3}$ and $K_2 = 6.4(1.1) \times 10^{-3}$. These values of K_1 and K_2 are very similar to the value of $K = 0.010(2)$ found for the i-QC $Ag_{50}In_{36}Gd_{14}$. It would thus appear that the spin dynamics are similar for these two spin glasses.

The best fits of the $T_{f_1}(f)$ and $T_{f_2}(f)$ data (figure 11) to the Vogel–Fulcher law (equation (4)), assuming $f_0 = 1 \times 10^{13}$ Hz, yield $E_a^1/k_B = 6.60(79)$, $T_0^1 = 3.41(4)$ K and $E_a^2/k_B = 2.56(41)$, $T_0^2 = 2.32(2)$ K, respectively. The values of r^2

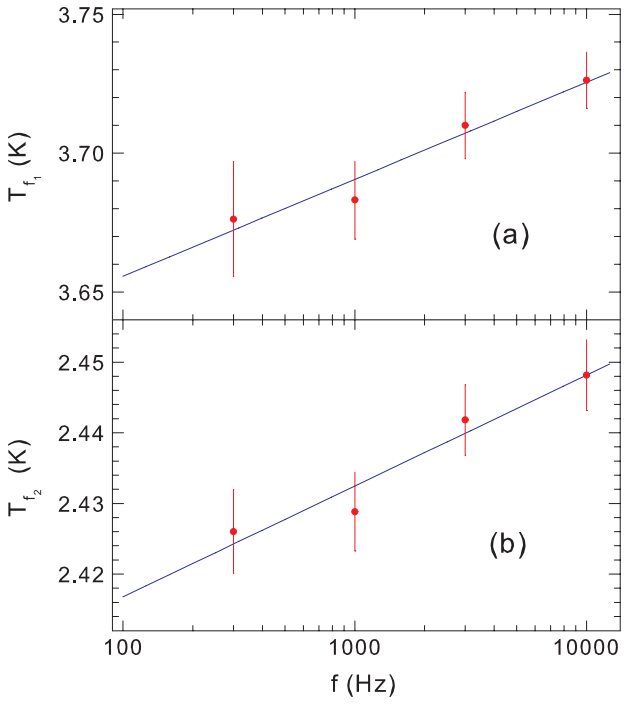

Figure 10. The frequency dependence of the freezing temperatures (a) T_{f_1} and (b) T_{f_2} for the 1/1 approximant $Ag_{50}In_{36}Gd_{14}$. The solid lines are the best linear fits to the data.

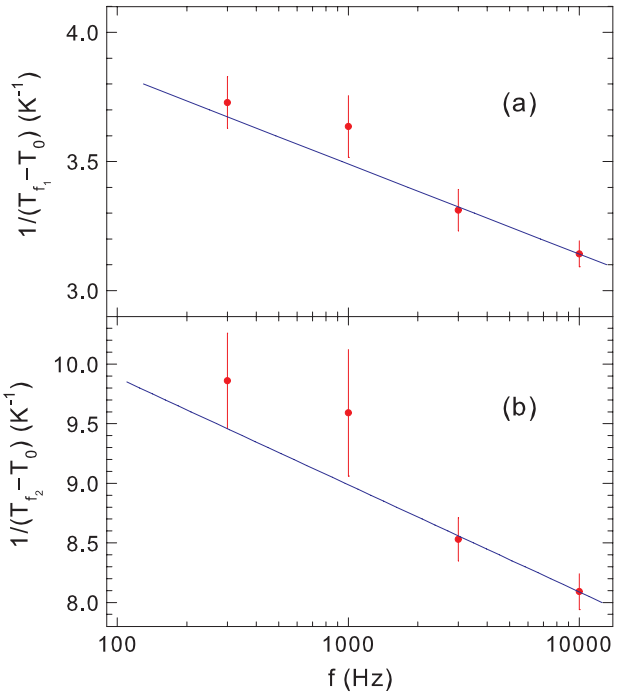

Figure 11. The frequency dependence of the freezing temperatures (a) T_{f_1} and (b) T_{f_2} for the 1/1 approximant $Ag_{50}In_{36}Gd_{14}$. The solid lines are the best fits to equation (4).

corresponding to these fits are, respectively, 0.9924 and 0.9879. As observed for other spin glasses [25], the parameters derived fulfil the inequality $T_0 < E_a/k_B$.

Figure 12 shows the fits of the $T_{f_1}(f)$ and $T_{f_2}(f)$ data to the power law (equation (5)), with the corresponding r^2

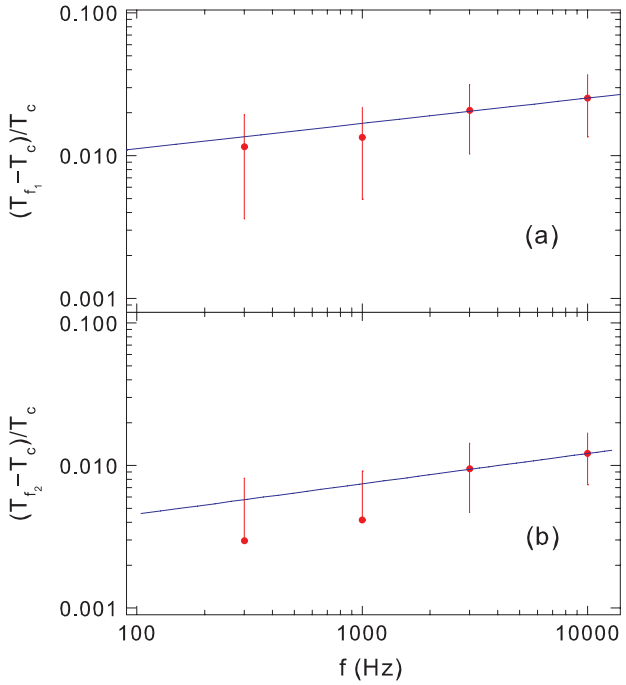

Figure 12. The frequency dependence of the freezing temperatures (a) T_{f_1} and (b) T_{f_2} for the 1/1 approximant $Ag_{50}In_{36}Gd_{14}$. The solid lines are the best fits to equation (5).

values of 0.9887 and 0.9802, respectively. The parameters derived from the fits, assuming that $f_0 = 1 \times 10^{13}$ Hz, are $T_c^1 = 3.63(2)$ K, $(z\nu)_1 = 5.64(30)$, and $T_c^2 = 2.42(1)$ K, $(z\nu)_2 = 4.70(25)$. The values determined for $z\nu$ are consistent with the values obtained for other spin-glass systems [21, 30].

Clearly, the values of r^2 are larger for the fits of the $T_{f_1}(f)$ and $T_{f_2}(f)$ data to equation (4) than to equation (5). This may be interpreted as evidence that the spin freezing in the 1/1 approximant $Ag_{50}In_{36}Gd_{14}$, similarly to the case for the i-QC $Ag_{50}In_{36}Gd_{14}$, is not a true equilibrium phase transition but rather a nonequilibrium phenomenon.

The presence of two distinct features in the $\chi'(T)$ and $\chi''(T)$ dependences (figures 8 and 9) is perhaps the most interesting aspect of the spin freezing phenomenon for the 1/1 approximant $Ag_{50}In_{36}Gd_{14}$. In virtually all known spin glasses, spin freezing is a one-stage process [21, 30]. It appears that spin freezing in the 1/1 approximant $Ag_{50}In_{36}Gd_{14}$ is occurring in two stages: at ≈3.6 K spins develop short-range correlations but they continue to fluctuate at low frequencies, and then long-range freezing is achieved upon further cooling to below ≈2.4 K. A similar two-stage freezing process has been observed for geometrically frustrated magnets, $Gd_3Ga_5O_{12}$, $Dy_{2-x}Yb_xTi_2O_7$, and $Ho_2Ti_2O_7$ [31–33].

The occurrence of a two-stage freezing process in the 1/1 approximant $Ag_{50}In_{36}Gd_{14}$ can possibly be related to its atomic structure. The atomic structure of the 1/1 approximant $Ag_{50}In_{36}Gd_{14}$ is the same as that of the 1/1 approximant $GdCd_6$ [7], with Ag/In atoms occupying the Cd sites. The atomic structure of the 1/1 approximant $Ag_{50}In_{36}Gd_{14}$ can thus be described as a body-centered-cubic arrangement of partially interpenetrating rhombic triacontahedral cluster

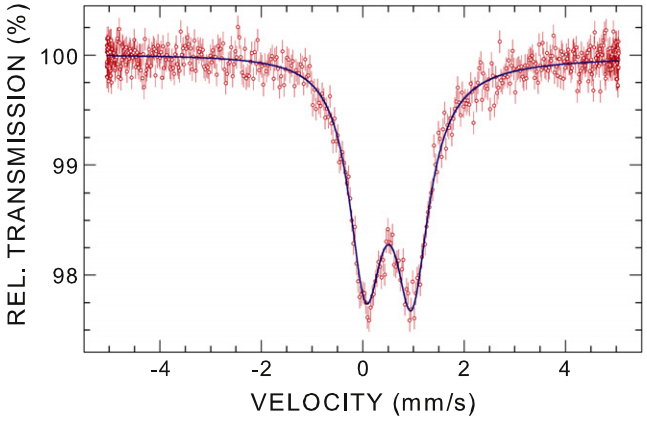

Figure 13. The ^{155}Gd Mössbauer spectrum of the 1/1 approximant $Ag_{50}In_{36}Gd_{14}$ at 4.6 K fitted (solid line) with an electric quadrupole hyperfine interaction. The zero-velocity origin is relative to the source.

units. The rhombic triacontahedral cluster consists of four successive shells: the inner Ag/In tetrahedron, the Ag/In dodecahedron, the Gd icosahedron, and the Ag/In icosidodecahedron. The location of magnetic Gd atoms at the vertices of the icosahedron is the source of frustration necessary for the occurrence of a spin-glass behavior. There are only two linkages between the neighboring triacontahedral clusters: one along the twofold axes and the other along the threefold axes [34, 35]. It follows that the same two linkages occur between the neighboring Gd icosahedra, and this may be related to the two-stage freezing process in the 1/1 approximant $Ag_{50}In_{36}Gd_{14}$

3.3. Mössbauer spectroscopy

Figure 13 shows the ^{155}Gd Mössbauer spectrum of the 1/1 approximant $Ag_{50}In_{36}Gd_{14}$ measured at 4.6 K, i.e., in the paramagnetic region above T_{f_1}. The Gd^{3+} ions are located at the site with the point symmetry m ... [7], which ensures a non-zero EFG at the Gd^{3+} site, and hence a non-zero electric quadrupole hyperfine interaction. The Mössbauer spectrum in figure 13 does indeed exhibit the presence of a substantial electric quadrupole hyperfine interaction and the absence of the magnetic dipole hyperfine interaction. The absence of the magnetic dipole hyperfine interaction in the Mössbauer spectrum in figure 13 proves that at 4.6 K the Gd spins are not in a frozen state. For ^{155}Gd nuclei, the quadrupole moment of the excited nuclear state $Q_{ex} = 0.12$ b [13] is significantly smaller than that of the ground nuclear state, $Q_g = 1.30$ b [36]. This causes the quadrupole splitting of the excited nuclear state, which is sensitive to the sign of V_{zz} and the magnitude of η, to be smaller than the natural linewidth $\Gamma_{nat} = 0.250$ mm s^{-1}. Consequently, only the absolute value of the effective quadrupole splitting parameter $\Delta_g^{eff} = eQ_g|V_{zz}|\sqrt{1+\eta^2/3}$ can be derived from a Mössbauer spectrum of a sample in the paramagnetic state [37]. The parameters derived from the fit ($\chi^2 = 1.11$) of the Mössbauer spectrum (figure 13) are: the isomer shift (relative to the ^{155}Eu($SmPd_3$) source) $\delta = 0.506(6)$ mm s^{-1},

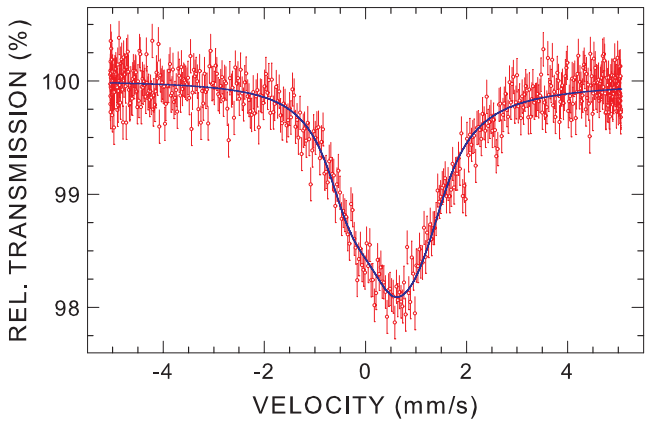

Figure 14. The ^{155}Gd Mössbauer spectrum of the 1/1 approximant $Ag_{50}In_{36}Gd_{14}$ at 1.5 K fitted (solid line) with combined magnetic dipole and electric quadrupole hyperfine interactions. The zero-velocity origin is relative to the source.

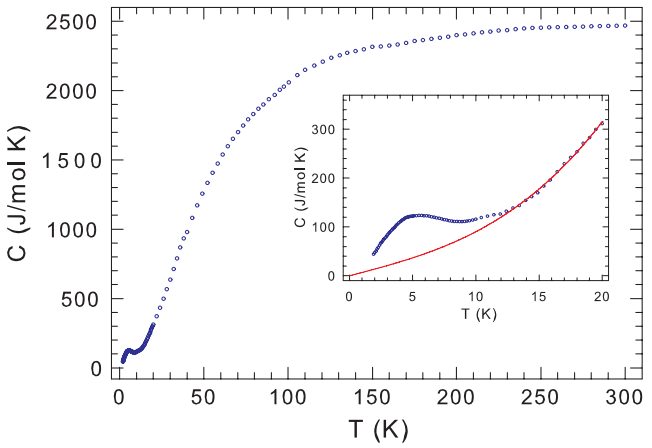

Figure 15. The temperature dependence of the specific heat of the 1/1 approximant $Ag_{50}In_{36}Gd_{14}$. The inset shows a magnification of the low-temperature region. The solid line is the fit to equation (7) of the specific heat data in the temperature range 13–20 K.

$\Delta_g^{\text{eff}} = 1.897(19)$ mm s^{-1}, $f_a = 10.3(1)\%$, and $\Gamma_a = 0.424(16)$ mm s^{-1}. The value of δ confirms the trivalent state of Gd in the 1/1 approximant $Ag_{50}In_{36}Gd_{14}$ [37]. The value of Δ_g^{eff} is close to that for the i-QC $Ag_{50}In_{36}Gd_{14}$ [9], which indicates a strong similarity of the local atomic structure around the Gd atoms in the 1/1 approximant and the i-QC $Ag_{50}In_{36}Gd_{14}$.

In terms of the Debye approximation of the lattice vibrations, the absorber Debye–Waller factor f_a is expressed [12] in terms of the Debye temperature, Θ_D, as

$$f_a(T) = \exp\left\{-\frac{3}{4}\frac{E_\gamma^2}{Mc^2k_B\Theta_D}\left[1+\left(\frac{T}{\Theta_D}\right)^2 \times \int_0^{\Theta_D/T}\frac{x\,dx}{e^x-1}\right]\right\}, \quad (6)$$

where E_γ is the energy of the Mössbauer transition, M is the mass of the Mössbauer nucleus, and c is the speed of light. The value of $f_a = 10.3(1)\%$ derived from the fit of the Mössbauer spectrum in figure 13 yields via equation (6) $\Theta_D = 199(1)$ K, which is the same as Θ_D for the i-QC $Ag_{50}In_{36}Gd_{14}$ [9]. This means that the phonon dynamics are very similar for these two alloys. The low value of Θ_D of the 1/1 approximant $Ag_{50}In_{36}Gd_{14}$ compares well with the value of 145.2 K for the 1/1 approximant $YbCd_6$ derived from the specific heat [38].

The ^{155}Gd Mössbauer spectrum of the 1/1 approximant $Ag_{50}In_{36}Gd_{14}$ at 1.5 K, i.e. below T_{f_2}, clearly shows (figure 14) the presence of combined magnetic dipole and electric quadrupole hyperfine interactions. The presence of the magnetic dipole hyperfine interaction in the Mössbauer spectrum in figure 14 proves that at 1.5 K the Gd spins are frozen. The Mössbauer spectrum in figure 14 was fitted by fixing the value of Γ_a to 0.424 mm s^{-1} obtained from the fit of the 4.6 K Mössbauer spectrum, and the value of θ to 0.0°. The parameters derived from the fit ($\chi^2 = 1.06$) of the Mössbauer spectrum (figure 14) are: $\delta = 0.483(18)$ mm s^{-1}, $H_{hf} = 137.3(11.8)$ kOe, the quadrupole splitting constant $eQ_gV_{zz} = 1.899(29)$ mm s^{-1} ($V_{zz} = 4.21(6) \times 10^{21}$ V cm^{-2}), $\eta = 0.2(2)$, and $f_a = 10.4(1)\%$. A substantial value of H_{hf} indicates a considerable magnetic moment of Gd atoms.

3.4. Specific heat

The temperature-dependent specific heat (C) data for the 1/1 approximant $Ag_{50}In_{36}Gd_{14}$ are shown in figure 15. At room temperature, C is 2469 J mol^{-1} K^{-1}. This is close to the value $3rR$ (r is the number of atoms per formula unit and R is the molar gas constant) of 2494 J mol^{-1} K^{-1} expected from the law of Dulong and Petit [20]. There is a broad maximum in C (inset in figure 15) at a temperature higher than T_f ($T_{max} \approx 1.3T_f$) and a gradual fall-off of C at increasing temperatures $T \longrightarrow 2.5T_f$. Such a temperature dependence of C around T_f has been observed for various spin glasses [21].

In order to determine the magnetic contribution C_m to the specific heat of the 1/1 approximant $Ag_{50}In_{36}Gd_{14}$, the electronic and lattice contributions were determined first by fitting the $C(T)$ data in the temperature range 13–20 K (inset in figure 15) to the equation

$$C(T) = \gamma T + \beta T^3, \quad (7)$$

where γ is the electronic specific heat coefficient and $\beta = \frac{12\pi^4 Rr}{5\Theta_D^3}$ is the lattice specific heat coefficient. The values of γ and β obtained from the fit are, respectively, 6.77(19) J mol^{-1} K^{-2} and 22.5(6) mJ mol^{-1} K^{-4}. This value of β corresponds to $\Theta_D = 205(2)$ K, which is very close to the value of 199(1) K inferred from the Mössbauer data.

The magnetic contribution to the specific heat for the 1/1 approximant $Ag_{50}In_{36}Gd_{14}$ obtained by subtracting the electronic and lattice contributions from C is shown in figure 16. It exhibits a broad maximum at ≈4.5 K. This temperature is about 30% higher than T_f. The fact that the temperature at which C_m reaches its maximum is larger than T_f (figure 16) agrees with what has been observed for many spin glasses [21]. Interestingly, the plot of C_m/T (=dS_m/dT, S_m being the magnetic entropy) as a function of temperature (figure 17) shows that the temperature at which C_m/T attains its maximum coincides with T_f. It would appear that in the 1/1 approximant $Ag_{50}In_{36}Gd_{14}$ spin glass the spin freezing is associated with a change in the magnetic

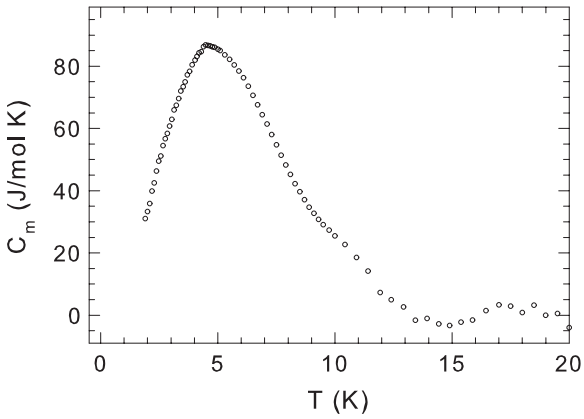

Figure 16. The magnetic contribution to the specific heat for the 1/1 approximant $Ag_{50}In_{36}Gd_{14}$ as a function of temperature.

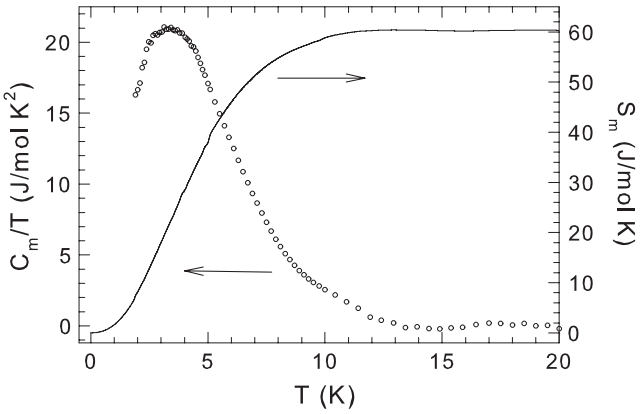

Figure 17. C_m/T as a function of temperature and the magnetic entropy S_m as a function of temperature for the 1/1 approximant $Ag_{50}In_{36}Gd_{14}$.

entropy (revealed by C_m/T) rather than with a change in the magnetic internal energy (revealed by C_m). A similar coincidence between the temperature at which C_m/T attains its maximum and T_f was observed in several spin-glass systems: $Pd_{1-x}Mn_x$ [39], $Cu_{1-x}Mn_x$ [40, 41], $Au_{1-x}Fe_x$ [41, 42], and i-QC $Al_{70}Mn_9Pd_{21}$ [43].

The temperature dependence of the magnetic entropy, $S_m = \int_0^T (C_m/T')\,dT'$, was calculated by integration of the C_m/T versus T dependence (figure 17), after an extrapolation of the C_m/T data down to the origin (i.e., for $T = 0$, $S_m = 0$). S_m saturates at 60.3 J mol^{-1} K^{-1}, which amounts to only 24.9% of the expected value $xR\ln(2J+1)$ (x is the number of atoms carrying the magnetic moment per formula unit) of 242 J mol^{-1} K^{-1}. The $S_m(T)$ dependence reveals (figure 17) that 63% of the entropy is released above T_f. This suggests that spin freezing at T_f removes only a small contribution to the magnetic entropy, and implies a significant short-range order of the magnetic moments above T_f.

4. Summary

Measurements of the dc and ac magnetic susceptibility, ^{155}Gd Mössbauer spectra, and specific heat of the 1/1 approximant $Ag_{50}In_{36}Gd_{14}$, and of the ac magnetic susceptibility of the icosahedral quasicrystal $Ag_{50}In_{36}Gd_{14}$ are reported. It is shown that these two alloys develop no long-range magnetic order, but are spin glasses. Freezing of Gd spins occurs at $T_f = 4.3$ K in the icosahedral quasicrystal $Ag_{50}In_{36}Gd_{14}$ and the frequency dependence of T_f can be described by means of the Vogel–Fulcher law and the power-law divergence. In the 1/1 approximant $Ag_{50}In_{36}Gd_{14}$, Gd spin freezing takes place in two stages: at $T_{f_1} = 3.7$ K Gd spins develop short-range correlations but continue to fluctuate, and then long-range freezing is achieved upon further cooling below $T_{f_2} = 2.4$ K. The dependences of T_{f_1} and T_{f_2} on frequency can be accounted for by the Vogel–Fulcher and power laws. It is argued that the spin freezing, in both alloys, is not a true equilibrium phase transition but rather a nonequilibrium phenomenon. The ^{155}Gd Mössbauer spectra of the 1/1 approximant $Ag_{50}In_{36}Gd_{14}$ confirm that the Gd spins are frozen at 1.5 K and are fluctuating at 4.6 K. The maximum in the magnetic specific heat occurs at a temperature that is 30% larger than T_{f_1}, but the temperature derivative of the magnetic entropy has a maximum at T_{f_1}. The Debye temperature of the 1/1 approximant $Ag_{50}In_{36}Gd_{14}$ is 199(1) K as determined from the Mössbauer data, and 205(2) K as determined from the specific heat data.

Acknowledgments

This work was supported by the Natural Sciences and Engineering Research Council of Canada. Support from the Polish Ministry of Science and Higher Education and the Structural Funds of the European Commission, Project No. SPO WKP 1.4.3, is gratefully acknowledged.

References

[1] Stadnik Z M (ed) 1999 *Physical Properties of Quasicrystals* (Berlin: Springer)
Suck J-B, Schreiber M and Häussler P (ed) 2002 *Quasicrystals, An Introductions to Structure, Physical Properties, and Applications* (Berlin: Springer)
[2] Tsai A P, Guo J Q, Abe E, Takakura H and Sato T J 2000 *Nature* **408** 537
Guo J Q, Abe E and Tsai A P 2000 *Phys. Rev.* B **62** R14605
[3] Guo J Q and Tsai A P 2000 *Phil. Mag. Lett.* **82** 349
[4] Iwano S, Nishimoto H, Tamura R and Takeuchi S 2006 *Phil. Mag.* **86** 435
[5] Elser V and Henley C L 1985 *Phys. Rev. Lett.* **55** 2883
[6] Takakura H, Guo J Q and Tsai A P 2001 *Phil. Mag. Lett.* **81** 411
[7] Gómez C P and Lidin S 2003 *Phys. Rev.* B **68** 024203
Gómez C P and Lidin S 2001 *Angew. Chem. Int. Edn Engl.* **40** 4037
[8] Ruan J F, Kuo K H, Guo J Q and Tsai A P 2004 *J. Alloys Compounds* **370** L23
[9] Stadnik Z M, Al-Qadi K and Wang P 2007 *J. Phys.: Condens. Matter* **19** 326208
[10] Bish D L and Chipera S J 1989 *Powder Diffract.* **4** 137
[11] Otterloo B F, Stadnik Z M and Swolfs A E M 1983 *Rev. Sci. Instrum.* **54** 1575
[12] Greenwood N N and Gibb T C 1971 *Mössbauer Spectroscopy* (London: Chapman and Hall)

Gütlich P, Link R and Trautwein A 1978 *Mössbauer Spectroscopy and Transition Metal Chemistry* (Berlin: Springer)
[13] Armon H, Bauminger E R and Ofer S 1973 *Phys. Lett.* B **43** 380
[14] Stadnik Z M and Zukrowski J 2005 unpublished
[15] Margulies S and Ehrman J R 1961 *Nucl. Instrum. Methods* **12** 131
Shenoy G K, Friedt J M, Maletta H and Ruby S L 1974 *Mössbauer Effect Methodology* vol 10, ed I J Gruverman, C W Seidel and D K Dieterly (New York: Plenum) p 277
[16] Young R A 1993 *The Rietveld Method* (Oxford: Oxford University Press)
[17] Goldman A I and Kelton K F 1993 *Rev. Mod. Phys.* **65** 213
[18] Selwood P W 1956 *Magnetochemistry* (New York: Interscience)
[19] Avila M A, Bud'ko S L and Canfield P C 2004 *J. Magn. Magn. Mater.* **270** 51
Sefat A S, Li B, Bud'ko S L and Canfield P C 2007 *Phys. Rev.* B **76** 174419
[20] Ashcroft N W and Mermin N D 1976 *Solid State Physics* (Philadelphia, PA: Saunders)
[21] Mydosh J A 1993 *Spin Glasses: An Experimental Introduction* (London: Taylor and Francis)
[22] Toulouse G 1977 *Commun. Phys.* **2** 116
Binder K and Young A P 1986 *Rev. Mod. Phys.* **58** 801
[23] Ramirez A P 2001 *Handbook of Magnetic Materials* vol 13, ed K H J Buschow (Amsterdam: Elsevier) p 423
[24] Fisher I R, Cheon K O, Panchula A F, Canfield P C, Chernikov M, Ott H R and Dennis K 1999 *Phys. Rev.* B **59** 308
[25] Tholence J L 1980 *Solid State Commun.* **35** 113
[26] Edwards S F and Anderson P W 1975 *J. Phys. F: Met. Phys.* **5** 965
[27] Shtrikman S and Wohlfarth E P 1981 *Phys. Lett.* A **85** 467
[28] Senyshyn A, Trots D M, Engel J M, Vasylechko L, Ehrenberg H, Hansen T, Berkowski M and Fuess H 2009 *J. Phys.: Condens. Matter* **21** 145405
[29] Hohenberg P C and Halperin B I 1977 *Rev. Mod. Phys.* **49** 435
[30] Souletie J and Tholence J L 1985 *Phys. Rev.* B **32** 516
[31] Schiffer P, Ramirez A P, Huse D A, Gammel P L, Yaron U, Bishop D J and Valentino A J 1995 *Phys. Rev. Lett.* **74** 2379
[32] Snyder J, Slusky J S, Cava R J and Schiffer P 2002 *Phys. Rev.* B **66** 064432
[33] Ehlers G, Cornelius A L, Fennell T, Koza M, Bramwell S T and Gardner J S 2004 *J. Phys.: Condens. Matter* **16** S635
[34] Takakura H, Gómez C P, Yamamoto A, de Boissieu M and Tsai A P 2007 *Nat. Mater.* **6** 58
[35] Lin Q and Corbett J D 2009 *Controlled Assembly and Modification of Inorganic Systems* ed X-T Wu (Berlin: Springer) p 1
[36] Tanaka Y, Laubacher D B, Steffen R M, Shera E B, Wohlfahrt H D and Hoehn M V 1982 *Phys. Lett.* B **108** 8
[37] Czjzek G 1993 *Mössbauer Spectroscopy Applied to Magnetism and Materials Science* vol 1, ed G J Long and F Grandjean (New York: Plenum) p 373
[38] Dhar S K, Palenzona A, Manfrinetti P and Pattalwar S M 2002 *J. Phys.: Condens. Matter* **13** 517
[39] Zweers H A, Pelt W, Nieuwenhuys G J and Mydosh J A 1977 *Physica* B **86–88** 837
[40] Martin D L 1979 *Phys. Rev.* B **20** 368
Martin D L 1980 *Phys. Rev.* B **21** 1902
[41] Martin D L 1987 *Phys. Rev.* B **36** 2147
[42] Martin D L 1980 *Phys. Rev.* B **21** 1906
Mirza K A and Loram J W 1985 *J. Phys. F: Met. Phys.* **15** 439
[43] Chernikov M A, Bernasconi A, Beeli C, Schilling A and Ott H R 1993 *Phys. Rev.* B **48** 3058